AD_____

Award Number: DAMD17-99-IA-9382

TITLE: Cell and Molecular Biology of Ataxia Telangiectasia Heterozygous Human Mammary Epithelial Cells Irradiated in Culture

PRINCIPAL INVESTIGATOR: Robert C. Richmond, Ph.D.

CONTRACTING ORGANIZATION: NASA/Marshall Space Flight Center
Marshall Space Flight Center, Alabama 35812

REPORT DATE: September 2002

TYPE OF REPORT: Final

PREPARED FOR: U.S. Army Medical Research and Materiel Command
Fort Detrick, Maryland 21702-5012

REPORT DOCUMENTATION PAGE

Form Approved
OMB No. 074-0188

1. AGENCY USE ONLY (Leave blank)	2. REPORT DATE	3. REPORT TYPE AND DATES COVERED
	September 2002	Final (1 Sep 99 - 31 Aug 02)

4. TITLE AND SUBTITLE
Cell and Molecular Biology of Ataxia Telangiectasia Heterozygous Human Mammary Epithelial Cells Irradiated in Culture

5. FUNDING NUMBERS
DAMD17-99-IA-9382

6. AUTHOR(S) :
Robert C. Richmond, Ph.D.

7. PERFORMING ORGANIZATION NAME(S) AND ADDRESS(ES)
NASA/Marshall Space Flight Center
Marshall Space Flight Center, AL 35812

E-Mail: robert.richmond@msfc.nasa.gov

8. PERFORMING ORGANIZATION REPORT NUMBER

9. SPONSORING / MONITORING AGENCY NAME(S) AND ADDRESS(ES)
U.S. Army Medical Research and Materiel Command
Fort Detrick, Maryland 21702-5012

10. SPONSORING / MONITORING AGENCY REPORT NUMBER

11. SUPPLEMENTARY NOTES
Original contains color plates: All DTIC reproductions will be in black and white.

12a. DISTRIBUTION / AVAILABILITY STATEMENT
Approved for Public Release; Distribution Unlimited

12b. DISTRIBUTION CODE

13. ABSTRACT *(Maximum 200 Words)*

The goal of this research is to define markers expressed in clinically normal human mammary epithelial cells (HMEC) such that a molecular epidemiological model of ionizing radiation-induced cancer may be considered. This approach has value since existing predictive models for radiogenic late effects have high uncertainty, and since tools of molecular biology have recently advanced such that molecular epidemiology is now a good investigative area for advancing predictive risk modeling.

Early markers related to carcinogenic pathway are identified for examination as panels of protein expression to be probed in HMEC in tissue culture irradiated or not with cesium-137 gamma rays. Panels of markers chosen relate to the dynamics of extracellular matrix, the architecture of the cell, and the repair of DNA-damage and control of cell proliferation. Marker-expression is determined as a function of age (passage number) and phase of growth (log versus plateau) of HMEC. Whereas any specific malignant cancer is likely to be of clonal origin, it is hypothesized that predictive value of some early markers reside in their widespread expression in populations of irradiated HMEC as field effects that promote selection of genetically altered cells providing the malignant phenotype.

It is found that expression of ATM gene product, p53, estrogen receptor, cytokeratin 18, and apparent apoptosis-related nuclear fragmentation are altered as field effects in irradiated HMEC, and may thus be considered for use in the assessment of carcinogenic risk of ionizing radiation.

14. SUBJECT TERMS:
breast cancer

15. NUMBER OF PAGES
24

16. PRICE CODE

17. SECURITY CLASSIFICATION OF REPORT	18. SECURITY CLASSIFICATION OF THIS PAGE	19. SECURITY CLASSIFICATION OF ABSTRACT	20. LIMITATION OF ABSTRACT
Unclassified	Unclassified	Unclassified	Unlimited

Table of Contents

INTRODUCTION

As a malignant phenotype within a given patient, radiogenic cancer traditionally is thought to arise from clonal expansion of a mutated cell derived from an initially surviving acutely damaged cell whose progeny then accumulate through successive lineages approximately 5 to 7 mutations in addition to the initiating acute genetic damage. Whereas the clonal origin of any given established primary metastatic cancer is likely, requirement for that clone being derived as a descendent of sequential mutations promoted from the initially damaged cell appears to be a dogma being shown as possibly inaccurate. Evidence is accumulating that an intervening selection process between radiogenic initiation and final clonal progression to metastatic disease may be promoted from field effects within the initially irradiated population.

Field effects are determined at variably early stages within an irradiated population. Field effects are anticipated to be predictive of cancer risk, and therefore may provide a dataset useful for early postirradiation estimation of such late effects.
Population field effects that can be so used are:
1) genomic instability, i.e., diverse cytogenetic variation developing within irradiated populations, where aneuploidy and accumulating chromosomal aberrations are thought to be prognostic of cancer risk;
2) bystander effect, i.e., epigenetic and genetic damage caused in cells of an irradiated population that are adjacent to those being effected with primary radiogenic damage, where this intercellular biochemical transduction is shown to be possibly prognostic of cancer risk, and breaks the dogma that clonally "dead" cells cannot be involved in subsequent formation of cancer.

Molecular epidemiology is considered to be alteration within the irradiated population of cells of expression of proteins bearing on and/or prognostic for cancer risk. Molecular epidemiology within A-T heterogeneous HMEC is a focus of this study of effects of Cs-137 gamma irradiation within two-dimensional populations grown to early confluence in tissue culture flasks. Categories of protein-expression were considered for study of early protein markers, these being proteins associated with DNA-repair and cell proliferation, with cytoskeleton, and with extracellular matrix. Related postirradiation alterations in apoptosis, multinucleation, and cell-cycle variation were also considered in these HMEC.

Individuals who carry two defective autosomal genes supporting the syndrome ataxia-telangiectasia (A-T) are prone to a number of clinical pathologies that relate to a reduced ability to repair DNA and chromosome damage in their cells. This damage can be either naturally created internally, such as by the normal rearrangement of DNA in immune cells responding to challenge by antigens, or externally created, such as by the local energy deposited by ionizing radiation. One long-term consequence of this lowered repair is a high rate of malignant cancers such that lymphomas and leukemias, for example, occur in excess of a hundred times more often in those with two defective genes than in those with nondefective genes. There are only about 600 recessive homozygotes of A-T in the United States, but about 1% of the entire population is estimated to be clinically silent heterozygous A-T carriers. Within a pedigree genetically defined for ataxia-telangiectasia, it has been shown with very high statistical significance that A-T heterozygous women develop breast cancer with incidence approximately 6 times that of the general population (12). It is reasonable to ask if cells from such A-T heterozygous individuals are susceptible to radiation-induced alterations indicative of carcinogenesis.

Ataxia-telangiectasia (A-T) is a radiation-sensitive autosomal genetic syndrome (1, 2) that broadly poses two levels of risk to the recipients of the A-T gene located on chromosome 11q22-23 (3) , that is, to those who are homozygous recessive (and clinically defined) and to those who are heterozygous (and clinically silent) for this gene. Fibroblasts and lymphoblastoid cells obtained from A-T homozygotes are relatively highly sensitive to radiation, and those cells obtained from A-T heterozygotes are often of intermediate radiation sensitivity (4-6). It is hypothesized that the exquisite radiation sensitivities of A-T homozygous cells will be reflected to some degree in the radiation responses established for A-T heterozygous human mammary epithelial cells (HMEC), and that this sensitivity will effect expression of carcinogenic process responsible for the known breast cancer susceptibility in women who are heterozygous for the A-T gene.

Three experimental Aims were proposed. First, focusing on A-T heterozygous breast cells, establish the relationship amongst postirradiation expression of markers believed to be involved in and/or relate to the molecular biology of cancer formation. Second, extend the same radiation studies to these A-T heterozygous breast cells that have additionally been genetically altered in ways that establish built-in steps in the known cancer producing pathway. Third, acquire additional specimens of breast tissue from A-T carrier women so that more cell isolates can be studied in replicate experiments and thereby test statistical significance of experimental findings.

This Final Report summarizes work applied to these Aims and results obtained. In brief, for Aim 1 methodology was developed and applied to study the expression of panels of proteins related to extracellular matrix, cell proliferation, and repair of DNA damage. For Aim 2, oncogenes E6 and E7 of Human Papalloma Virus-Type 16 were inserted into A-T heterozygous HMEC in collaboration with the laboratory of Dr. Ray White at the University of Utah, but level of effort has not been adequate to evaluate those immortalized cells within the panel of protein expression detailed in Aim 1. For Aim 3, a second A-T heterozygote breast tissue harvest in February of 2000 successfully added to the existing repository of A-T heterozygous breast cell isolates, but level of effort has not been adequate to further evaluate those isolates, and additional breast tissue harvests have not been obtained from A-T heterozygotes due to reduced NIH support to Dr. Mike Swift that had sustained his collaborative efforts in identifying for us A-T heterozygotes undergoing mastectomies from within his extensive epidemiologic database.

BODY

This Army IDEA grant was used to leverage the purchase of a Becton Dickinson FACSCalibur flow cytometer that was applied to cell cycle experiments performed within the scope of the Specific Aims of this proposal. Results provided by this flow cytometer significantly contributed to the potential breakthrough in cancer risk estimation that is summarized in the following paragraph.

Materials and Methods

Organoids were plated without prior freezing from harvests from both breasts into a total of 100mm polystyrene tissue culture dishes containing serum-free MEGM, and were grown in air/5% CO_2 at 37° C in standard fashion (8) . Primary outgrowth from these approximately 150 separately attached organoids contained both epithelial cells and fibroblasts. Fibroblast outgrowth was removed after the first 12 days of outgrowth from all dishes by extensive treatment with 0.2% bovine trypsin (Sigma) in Dulbecco's phosphate buffered saline without calcium or magnesium (PBS) followed by a two-fold rinse with PBS. Attached organoids and epithelial cells were impervious to this trypsinization. No additional fibroblasts were observed in any subsequent cultures, which were continued in serum-free MEGM.

Outgrowth and expansion of mixed HMEC populations approached late log-phase repeatedly, and this process was maintained in the original culture dishes by use of repeated partial trypsinization using saline-trypsin-versene (STV) preparation previously described (8) . STV dissociates HMEC attached to dish or flask surfaces into single cells. Partial trypsinizations were required approximately every 10 days, and involved incubation at 37° C for about 2 min followed by continued trypsinization at room temperature with continual microscopic observation until about 80% of the HMEC population was detached. Plates were then rinsed once with PBS containing 1 mg/ml soybean trypsin inhibitor (Sigma) and refed with MEGM for continued incubation. By the 4th partial trypsinization, morphological appearance of presumptive long-term growth HMEC (LTG HMEC), as previously described (8) was observed, and this cell type was isolated as a collection from all outgrowth dishes into an apparent pure culture following the 6th partial trypsinization. This LTG HMEC isolate was termed WH612/3 pass 1, and was expanded to provide pass 3, which became the frozen working stock for experiments here that work with pass 5 through 8.

Stromal fibroblasts were grown from the initial collagenase digestion of tissue that was collected separately from organoids. These were readily cultured in alpha-MEM without nucleosides or nucleotides (Sigma) supplemented with 10% defined nonheat-inactivated fetal bovine serum (FBS)

(HyClone). This fibroblast isolate was termed WSt718 pass 0, which was then trypsinized at late log-phase and expanded once to provide pass 1, which became the frozen working stock for experiments here that work with pass 3 through 6. Cryogenic preservation of WSt718 stromal fibroblasts and WH612/3 epithelial cells followed previously reported procedure (8) .

The work centered on long-term growth HMEC, i.e., with senescence occurring at approximately passage 13, that were isolated from a 41 year-old white female heterozygous for A-T. Tissue harvest required a total of 3 days, and followed established procedure based upon collagenase Type I (Sigma) disaggregation (8), except that whole tissue was minced and collagenase-dissociated using a modified method (9) because initial tissue reduction around organoids by mechanical scraping was not possible due to advanced breast disease presenting as extensive fibrosis. This patient was an obligate heterozygote for the autosomal recessive syndrome ataxia-telangiectasia (A-T) who donated tissue from both her prophylactic bilateral mastectomies, which were determined by extensive histopathology to be free of cancer. This individual was located by Dr. Mike Swift through his extensive database of individuals related to A-T children (7). Dr. Swift and coworkers additionally identified the specific ATM gene mutation in KW to be a GT deletion at nucleotide 7011 of exon 50 causing then truncation of the ATM gene protein (personal communication)..

Breast tissue harvest was also collected from a second obligate A-T heterozygote and harvested. The surgery providing this specimen was also identified by Dr. Mike Swift. This specimen was a single mastectomy obtained from a 32 year-old white female. Approximately 25% of initial tissue had been removed for use by surgical pathology. The specimen was anticipated to be noncancerous, and indeed the patient had elected prophylactic mastectomy at the time of her operation scheduled for removal of the contralateral breast known to be cancerous. However, the prophylactic specimen was subsequently determined to have central regions of infiltrating globular ductal carcinoma as well as ductal carcinoma in situ. Harvest of this tissue has to date led to isolation of organoids, overlying skin fibroblasts, and stromal fibroblasts. Organoids have yet to be cultured for isolation of long-term growth HMEC.

Two presumably normal control cultures were obtained for study. First was the LTG HMEC cell isolate 48R obtained at pass 14 from Dr. Martha Stampfer chosen to match the rapid 16 hr doubling time noted for WH612/3 HMEC. Second was the LTG HMEC cell isolate AG11132A obtained at pass 19 from the Corielle Cell Repository in Camden NJ, where that isolate was also provided by Dr. Martha Stampfer. It is noted that WH612/3 HMEC senesces at about pass 14, whereas 48R and AG11132A are expected to senesce at approximately pass 25. The difference in time of senescence may relate to difference in telomere lengths reflecting harvest from a 41 year old for WH612/3 and from ca. 18 year old women for 48R and AG11132A. All HMEC for these studies were grown in serum-free media as previously specified (8).

An early problem encountered in this study was the finding that immunostaining of WH612/3 HMEC in standard 2-dimensional tissue culture often led to false negatives using an antimouse-IgG polyclonal antibody mixture as the nonspecific primary antibody control. Although use of a monoclonal IgG antibody known not to have a matching epitope, such as anti-bromodeoxyuridine, did not provide false negative controls for immunostaining, it was felt necessary to establish adequate negative control staining using the broadspectrum anti-IgG. To this end much effort was devoted, and success ultimately achieved by the inclusion of 1% Tween-20 detergent (vol/vol) in all solutions of immunostaining procedure except final staining with diaminobenzidine (DAB). It was assumed that the dorsal extracellular matrix observed to be produced early-on in the growth of these attached HMEC acted to impede free solvent exchange of nonspecific primary and secondary antibodies used in immunostaining, and that Tween-20 acted to facilitate this exchange with the aqueous solvent.

A relatively broad panel of 21 primary antibodies for immunostaining was initiated for studies of protein expressions in nonirradiated HMEC as a function of phase of growth (early log, late log, early confluence, late confluence) and of cell age (passages 7 through 11). For immunostaining of nonirradiated cells, 1000 HMEC per well were plated in 96-well plates. Immunostaining of early log phase cells commenced approximately 2 days after plating, where phase of growth was established by repeated microscopic examination. The four levels of phase of growth were established within 96-

well plates prepared from each passage, where passages 8 through 11 were accumulated within 100 mm dishes. This panel contained the following primary antibodies.

TABLE 1:

	abbreviation	target	Indication
1	JIgG	mouse IgG (Jackson Labs)	negative control
2	BUdR	bromodeoxyuridine	negative control
3	FN	fibronectin	positive control & ECM
4	CS	chondroitin sulfate	extracellular matrix (ECM)
5	Col IV	collagen IV	extracellular matrix (ECM)
6	Col VII	collagen VII	extracellular matrix (ECM)
7	Lam	laminin	extracellular matrix (ECM)
8	C19	cytokeratin 19	cytoskeletal filament
9	C18	cytokeratin 18	cytoskeletal filament
10	CK14	cytokeratin 14	cytoskeletal filament
11	CK8	cytokeratin 8	cytoskeletal filament
12	CK5	cytokeratin 5	cytoskeletal filament
13	IGFR	insulin-like growth factor receptor	differentiation marker
14	ER	estrogen receptor	differentiation marker
15	FSP	fibroblast specific protein	differentiation marker
16	Lac	alpha-lactalbumin	differentiation marker
17	p53	p53	DNA repair & control
18	ATM-short	ataxia-telangiectasia short-length	DNA repair & control
19	ATM-long	ataxia-telangiectasia long-length	DNA repair & control
20	HS25	heat shock 25	stress response
21	HS70	heat shock 70	stress response

From the results using the initial panel of 21 primary antibodies, a second panel of 13 primary antibodies was selected for extended studies on cells irradiated with 30 rad, 60 rad, and 90 rad. For immunostaining of irradiated cells, 1000 HMEC per well were plated in 96-well plates. Immunostaining of early log-phase cells commenced 2 to 3 days after plating, where phase of growth was established by repeated microscopic examination. This panel contained the following primary anitbodies.

TABLE 2:

	abbreviation	target	Indication
1	JIgG	mouse IgG (Jackson Labs)	negative control
2	FN	fibronectin	positive control & ECM
3	CS	chondroitin sulfate	extracellular matrix (ECM)
4	Col IV	collagen IV	extracellular matrix (ECM)
5	Col VII	collagen VII	extracellular matrix (ECM)
6	Lam	laminin	extracellular matrix (ECM)
7	C19	cytokeratin 19	cytoskeletal filament
8	C18	cytokeratin 18	cytoskeletal filament
9	IGFR	insulin-like growth factor receptor	differentiation marker
10	ER	estrogen receptor	differentiation marker
11	p53	p53	DNA repair & control
12	ATM-short	ataxia-telangiectasia short-length	DNA repair & control
13	ATM-long	ataxia-telangiectasia long-length	DNA repair & control

For irradiation, HMEC were grown at pass 7 in T25 flasks to late-log phase and irradiated with a Shepherd Cs-137 open-beam irradiator at source-to-sample distance providing 1000 R/min with good dose distribution across the flasks. Dose levels for studies were standardized at 0, 30, 60, and 90 rads, where 100 rad is equal to one gray (Gy) in SI-units. Following irradiation, flasks were incubated further for 24 hr, and then passed 1:20 within T25 flasks, and additionally split to 96-well plates at a density of 1000 cells/well for 0 and 30 rad dose-levels, and at 2000 cells/well for 60 and 90 rad dose levels. Increased cell density plated for the two higher dose levels were required due to notably decreased growth rate for the initial post-irradiation split to 96-well plates. Splits to 96-well plates for all subsequent passages, i.e., 9 through 11, were done at the standard 1000 cells/well for all dose levels. The four levels of phase of growth were established within 96-well plates for each passage, where passages 8 through 11 were accumulated within T25 flasks.

Photomicrographs of both nonfluorescent and fluorescent images were recorded digitally using a Leitz Fluovert inverted microscope or a wide-angle Leitz Aristoplan research microscope. Specific immunofluorescence was achieved using antibody-directed procedures and methods associated with a variety of kits from Vector and Boehringer Mannheim. Directed fluorescence was achieved using DNA-intercalating dyes such as propidium iodide following established procedures. A Becton Dickenson 3-color FACSCalibur flow cytometer was obtained during the course of these studies, and was applied for both phenotypic expression of apoptosis and for determination of information relating to cell cycle for these HMEC, including cell cycle-phase distributions, hypoploidy inferring apoptosis, hyperploidy inferring incomplete cytokinesis and/or genomic instability, and aneuploidy inferring genomic instability.

The observation of apparent multinucleation in irradiated HMEC raised questions of related apoptosis in the context of the well known involution that occurs naturally in HMEC during life cycles in situ. Accordingly, a set of growth factor-deprivation experiments were performed with HMEC wherein required supplements to basal serum-free media were withheld, these factors being insulin, hydrocortisone, and bovine pituitary extract. The ensuing profound effects on multinucleation and TUNEL-positive reaction commonly associated with apoptosis were then examined by use of nonfluorescent and fluorescent microscopy and by flow cytometry (FCM).

KEY RESEARCH ACCOMPLISHMENTS

Experimental Results

1. Immunogenic Staining and Radiogenic Homeostatic Disequilibria

Systematic immunostaining of nonirradiated cultures of HMEC revealed some distinctions of marker-expression based upon cell phase, cell age, and specific HMEC isolate. Estrogen receptor (ER) in one experiment (not shown) was expressed more in log-phase than plateau-phase A-T heterozygous WH612/3 HMEC. However, in another experiment with these HMEC (Figure 1) nuclear expression of ER was determined for nonirradiated confluent but not log-phase cells, and irradiation caused dose-dependent increase in cytoplasmic expression of ER. Fibronectin was uniquely expressed extensively as extracellular matrix in early log-phase HMEC and consistently thereafter in all cultures (not shown), explaining its use as the positive control included in all immunostaining experiments (Tables 1 and 2). p53 was expressed preferentially in plateau-phase HMEC in the nucleus of AG11132A control cells (Figure 2), but in the cytoplasm of log-phase WH612/3 cells (Figure 3). Irradiation of late log-phase HMEC was seen to lead to notably increased expression of p53 in plateau-phase but not log-phase WH612/3 cells during extended postirradiation passage and culturing. It is notable that p53 expression in A-T heterozygous HMEC was found in the cytoplasm preferentially, regardless of irradiation exposure, compared to expression in the nucleus preferentially of presumably normal AG11132A HMEC, and that those irradiated cells demonstrated moderate dose-dependent decrease in p53 expression. **(Figures 2 and 3)**.

ATM gene-derived short-length protein staining provided preliminary finding of decreased expression in extended postirradiation cultures of AG11132A cells **(Figure 4)**, but comparative study of this radiogenic marker is not yet done for WH612/3 HMEC. The epitope for short-length anti-ATM protein monoclonal antibody (mAb) is in the first quarter of that phosphoinositol kinase, whereas the GT-deletion mutation causes a truncation mutation in the last quarter of that protein. Therefore, short-

length immunostaining provides potential homozygous expression-levels in both the normal and A-T heterozygous HMEC studied. A long-length anti-ATM kinase mAb that acts on epitope beyond the truncation mutation in WH612/3 HMEC has recently been applied to these studies in order to discriminate titers of ATM-expressed protein between the control and A-T heterozygous HMEC isolates.

At this time, the intermediate filament protein cytokeratin 18 (CK18) is relatively best established as being altered in its expression within irradiated populations of WH612/3 HMEC. As shown in Figures 5-7, CK18 expression in nonirradiated cells increases with increasing cell density (and less clearly with increasing cell passage). Also shown in Figures 5-7, populations of passaged irradiated cells persistently demonstrate dose-dependent increase of CK18 within log- and late-log-phase populations, but not obviously within confluent populations. Comparative studies on AG11132A control HMEC have not yet been completed.

2. Multinucleation and Morphometric Analysis

Microscopic observations of nonirradiated and irradiated HMEC revealed that increasing frequency of apparent multinucleation was occurring in irradiated cells as a function of both increasing radiation dose and age of population, i.e., postirradiation passage number. Counts of nuclei within cells presenting within random microscopic fields of advanced age (passage 11) of the control plus three radiation dose exposures were tabulated. That tabulation plus a photomicrograph of frequently observed clustering of multinucleation in populations of HMEC initially exposed to 90 rad is presented in Figure 8. Whereas multinucleation is typically assumed to be failed cytokinesis and end-stage cell viability, this apparent clonal expression of multinucleated irradiated cells raises a possibility that this persistent morphometric marker might also be prognostic for carcinogenic risk in these HMEC. The bizarre appearance of late passage WH612/3 HMEC generally, and especially following irradiation, raises issue for the extent to which apoptosis may be present in aging populations. It is interesting that apoptosis in HMEC has been reported not demonstrable by chromogenic TUNEL immunostaining, but is demonstrable by anti-annexin V immunostaining (13). In our hands, chromogenic TUNEL immunostaining using DAB also did not demonstrate apoptosis, but the more direct fluorogenic TUNEL immunostaining using FITC-conjugated primary mAb did show positive reaction within apparent multinuclei of these HMEC. It is known that cessation of lactation will lead to apoptosis-mediated massive involution of HMEC in breast tissue, and it was thus decided to examine multinucleation patterns in these HMEC following removal of growth factors from the serum-free growth media MEGM used for standard tissue culture. For this purpose the serum-free basal media MEBM from Clonetics was used directly for culture of WH612/3 HMEC, i.e., without addition of insulin, hydrocortisone or pituitary extract. Widespread apparent multinucleated cells were soon observed specifically in MEBM, as shown in Figure 9, and these apparent multinuclei uniformly demonstrated marked TUNEL-positive fluorescence immunostaining as shown in Figure 10. Initial study by flow cytometry of MEBM-grown HMEC trypsinized from cultures known to contain a high fraction of cells with apparent multinuclei did **not** reveal a substantial fraction of hyperploid cells (Figure 11). This absence of a hyperploid population is one reason why the term "apparent multinuclei" is used to describe this presumed apoptosis-driven condition.

3. Cell-Cycle and Cytogenetic Analyses

Genomic instability is one prognostic for carcinogenic process in mammalian cells (11). The acquisition of the FACSCalibur flow cytometer during Year 1 of this study allowed ploidy to be readily determined within the same DNA histograms established for the cell cycle analyses compiled for completion of specific aims of this work within populations of breast-derived cells being studied. Hypoploidy suggestive of apoptosis was at times observed, development of a hyperploid subpopulation of HMEC with increasing passage was repeatedly seen, and a consistent aneuploidy for both HMEC and autologous fibroblasts relative to the diploid human blood monocyte controls was obtained from these cell-cycle DNA histograms. We therefore extended our original set of Aims to correlate the meaningfulness of aneuploidy observed from FCM analysis to that obtained by cytogenetic analysis; we reported these cytogenetic findings in our Year 1 progress report, and were told that we had broken our research agreement with the Army and to stop further efforts regards cytogenetic experiments. Nonetheless, that initial cytogenetic study confirmed agreement with aneuploidy determined by FCM within the A-T heterozygous breast cell harvest such that 9%

aneuploidy for passage 3 stromal fibroblasts was obtained by both FCM (Figure 12) and cytogenetic analysis (Table 3), and for WH612/3 HMEC 89% cytogenetic aneuploidy for passage 8 determined by chromosome count (Table 3) corresponded to a ca. 30% aneuploidy of DNA content determined by FCM analysis for both WH612/3 and AG11132A HMEC (Figure 13). Plateau-phase cell-cycle histograms established for successive passages of WH612/3 HMEC following irradiation of pass 7 cultures show progressive accumulation of cells in G2/M coincident with emergence of a significant hyperploid population. These metrics of genomic instability may be meaningfully correlated with p53, ATM gene expression, and CK18 radiation-induced field effects described above.

Techniques for preparing metaphase spreads from autologous noncancerous cells isolated from human breast tissue followed previously established methods for leukocyte (10) modified for use with these attached cells.

ADDITIONAL KEY RESEARCH ACCOMPLISHMENTS

1. Extracellular matrix

a. Unique findings of cell-density dependent production in WH612 HMEC of exceedingly thin dorsal matrix at times leading to detachment and establishment of floating rafts of growing HMEC attached to the undersurface of the basement membrane-like matrix sheet. This is the first known observation in culture of a basement membrane-like extracellular matrix.

b. Unique findings of cell-density dependent production in WSt718 fibroblasts of contractile thick mucinous matrix leading always at late confluence to severe circumfrential retraction coincident with detachment of the cell sheet from the plastic surface, and formation then of a tight central rubber-like ball of cells and matrix attached via residual contacts to the plastic surface of the dish. This is the first known comparative difference noted in culture between HMEC and autologous fibroblasts in culture.

c. Vimentin, fibronectin, proteoglycan sulfate, and laminin, but not collagen IV are markers identified with WH612/3 HMEC as they progress into plateau phase. This marked absence of collagen IV in HMEC extracellular matrix is unusual. The presence of vimentin suggests possible initiation of epithelial-mesenchymal transition for these HMEC. The presence of alpha-actin in these HMEC could serve to support the possibility of such transition.

d. Fibronectin is expressed preferentially in early log phase WH612/3 HMEC and is rapidly and extensively exported from those cells to the surface of the growth plate in apparent initiation of matrix formation.

2. Cell proliferation and DNA-repair markers

a. Unique findings of age (pass)-dependent expression and/or cell density (growth phase)-dependent expression

1) Estrogen Receptor (ER) is expressed in WH612/3 HMEC preferentially in plateau-phase cells.
2) Insulin-like Growth Factor Receptor (ILGFR) is expressed coincident with ER.
3) p53 is expressed preferentially in the nucleus of AG11132A HMEC, but in the cytoplasm of WH612/3 HMEC.

3. Cytoskeletal CK markers

a. Unique findings of passage-age dependent expression and/or cell-density dependent expression in HMEC

1) CK18,14,5,19
2) alpha-Actin is expressed in WH612/3 HMEC suggesting phenotypic relationship with basal myoepithelial cells, and/or perhaps suggesting possible initiation of epithelial-mesenchymal transition for these HMEC in line with their coincident expression of vimentin noted above.

4. The first cytogenetic comparison of low-passage autologous stromal fibroblasts and HMEC was established from noncancerous human breast tissue. The incidence of cytogenetic aberrations was greater than expected in both cell types, and much more pronounced in HMEC, suggesting the possibility of a preferential genetic instability in epithelial tissue versus

stromal tissue due to their A-T heterozygous genotype. The approximate 9-fold excess of cytogenetic aberrations in HMEC compared to stromal fibroblasts raises the possibility that genetic instability may contribute to cancer susceptibility in A-T heterozygotes.

5. Establishment of the first human A-T heterozygous breast tissue cell repository.

REPORTABLE OUTCOMES

1. Culture and Cytogenetics of Noncancerous Human Mammary Cells Isolated from Ataxia-Telangiectasia Heterozygous Tissue; Robert Richmond, Ranjini Kale, and Olive Pettengill; in preparation.

2. Macromolecular field effects within irradiated populations of breast-derived cells; Robert Richmond, Karen Bors, Angela Cruz; in preparation

CONCLUSIONS

Experimental work designed to investigate mechanism-associated markers of radiogenic cancer has been the central focus of this study. To this end, it was first asked: What are the early events in an irradiated population of cells that might reasonably be considered as markers for predicting ultimate cancer risk? Although there are a number of early markers of cancer to be considered, the novel and valuable aspect of the question just posed is "early events", not markers per se. Early events are a dynamic of expression of early markers, whereas early markers alone are a static collection of proteins. Importantly, the developing field of functional genomics has provided an awareness that pathologies, including cancer, reflect complex shifts in equilibria of gene expression effected through both genetic and epigenetic pathways. It follows that the static markers touted to have meaning for understanding carcinogenesis are likely only a small representation of all events involved in carcinogenesis. This awareness supports the recent acceptance of macromolecular field effects as additions to the fundamental dogma of step-wise mutations progressing through successive progenies to generate the ultimate clonal origin of any established carcinoma. Two macromolecular field effects are already hypothesized in the literature to influence radiogenic cancer risk, and these are 1) genomic instability and 2) bystander effects. The molecular epidemiological study conducted here with A-T heterozygous HMEC has introduced a third field effect, where that dynamic process is now termed homeostatic disequilibria (HD), and is reflected by broad shifts in marker expressions within treated populations of cells as a function of phase of growth and age of the cell populations after treatment. Implicit in expression of HD is the assumption that the limited number of marker proteins selected for study in truth may or may not have substantial cause-effect relatedness to cancer risk, but do at least serve to indicate genomic disequilibria involving many nondetected gene products, i.e., nascent markers, that in total serve to provide altered selection pressures contributing to the rate of the multimutational pathways ultimately providing the lineage that expresses clonally derived metastatic disease. It is proposed that HD provides altered population selection pressure that accelerates the process of carcinogenesis, and that is additional to the dogma of multimutational pathways considered as fundamental to the clonal origin of cancer. Macroscopic clinical field effects are well recognized for underlying certain cancers, most notably bladder cancer and squamous cell cancer of the head-and-neck, where within the field of affected tissue unrelated multiple primaries develop to thwart efforts of local therapeutic management. It is suggested that these phenotypic clinical field-effect cancers serve to emphasize the outcome of the risk associated with the early events of HD macromolecular field effects.

The outcomes of this study regards changes in radiation-induced alterations in the field effects of protein marker expression have potential significance for improved risk-estimation of malignant transformation. Homeostatic disequilibria (HD) was demonstrated in extended cultures of A-T heterozygous HMEC such that increased growth phase-dependent expressions of cytokeratin 18 (CK18) and cytoplasm p53 was increased, and that HD correlated with cell age- and radiation dose-dependent expression of multinucleation. In addition, cell age-dependent, but not radiation-dependent, accumulation of G2/M and hyperploid fractions were shown to contribute to a composite context for the consideration of radiation-induced field effects. It is believed that this work is the first to

demonstrate radiation-induced field effects regards altered expression of proteins maintained within long-term continuance of irradiated populations. The proteins determined in this study to be altered in long-term expression are markers of significance for cancer progression and management. Therefore, a new hypothesis emerges from this study – that is, the equilibrium of proteomics defining and preserving the noncancerous state is altered as a consequence of radiation-induced field effects, thus providing broad alteration in subsequent selection pressure that supports then relatively rapid progression to an ultimate clonally derived carcinoma. Therefore, the long-standing conundrum of matching expected low frequencies of multistep-wise successively mutated progenies leading to the relatively high clinical frequencies of observed metastatic cancer might be resolved by further investigations on radiation-induced field effects within irradiated populations of cells and tissues. Potentially, a new area of risk assessment of radiogenic cancer has been introduced in this study.

Genetic instability studies need to be included in Aims extending from this work. Differences between autologous fibroblasts and HMEC from A-T heterozygous breast tissue need to be a comparative focus of studies on genetic instability.

Repositories of cells isolated from additional A-T heterozygous breast tissue need to be established for intercomparisons. The number of control HMEC isolates likewise need to be increased to validate better the findings of this work to date.

Extending and repeating these field effect studies on expression of markers of carcinogenesis needs to be a focus of continuing investigation.

REFERENCES

1. K. Sasai, J. W. Evans, M. S. Kovacs and J. M. Brown, Prediction of human cell radiosensitivity: comparison of clonogenic assay with chromosome aberrations scored using premature chromosome condensation with fluorescence in situ hybridization. *Int J Radiat Oncol Biol Phys* 30:1127-1132 (1994).
2. R. A. Gatti, Speculations on the ataxia-telangiectasia defect. *Clin Immunol Immunopathol* 61:S10-15 (1991).
3. K. Savitsky, A. Bar-Shira, S. Gilad, G. Rotman, Y. Ziv, L. Vanagaite, D. A. Tagle, S. Smith, T. Uziel, S. Sfez and et al., A single ataxia telangiectasia gene with a product similar to PI-3 kinase [see comments]. *Science* 268:1749-1753 (1995).
4. C. M. West, S. A. Elyan, P. Berry, R. Cowan and D. Scott, A comparison of the radiosensitivity of lymphocytes from normal donors, cancer patients, individuals with ataxia-telangiectasia (A-T) and A-T heterozygotes. *Int J Radiat Biol* 68:197-203 (1995).
5. T. K. Pandita and W. N. Hittelman, Increased initial levels of chromosome damage and heterogeneous chromosome repair in ataxia telangiectasia heterozygote cells. *Mutat Res* 310:1-13 (1994).
6. M. A. Hannan, F. Khougeer, Z. Halees, A. M. Sanei and B. A. Khan, Increased radiosensitivity and radioresistant DNA synthesis in cultured fibroblasts from patients with coronary atherosclerosis. *Arterioscler Thromb* 14:1761-1766 (1994).
7. M. Swift, D. Morrell, R.B. Massey, and C.L. Chase, Incidence of cancer in 161 families affected by ataxia-telangiectasia. *N. Engl. J. Med.* 325:1831-1836 (1991).
8. M.R. Stampfer, Isolation and growth of human mammary epithelial cells. *J. Tiss. Cult. Methods* 9:107-115 (1985).
9. J.J. Gomm, P.J. Browne, R.C. Coope, Q.Y. Liu, L. Buluwela, and R.C. Coombes, Isolation of pure populations of epithelial and myoepithelial cells from the normal human mammary gland using immunomagnetic separation with Dynabeads. *Analyt Biochem* 226:91-99 (1995).
10. P.S. Moorhead, P.C. Nowell, W.J. Mellman, D.M. Battips, and D.A. Hungerford, Chromosome Preparations of Leucocytes Cultured from Human Peripheral Blood. *Exptl. Cell Res.* 20: 613-616 (1960).
11. M.A. Nowak, A.L. Komarova, A. Sengupta, P.V. Jallepalli, l-M. Shih, B. Bogelstein, C. Lengauer, The role of chromosomal instability in tumor initiation. *Proc. Natl. Acad. Sci USA* Early Edition www.pnas.org/cgl/dol/10.1073/pnas.202617399 (2002).

12. P. Athma, R. Rappaport, M.Swift, Molecular genotyping shows that ataxia-telangiectasia heterozygotes are predisposed to breast cancer. *Cancer Genet Cytogenet* 92:130-134 (1996).
13. S.R. Romanov, B.K. Kozakiewicz, C.R. Holst, M.R. Stampfer, L.M. Haupt, T.D. Tisty, Normal human mammary epithelial cells spontaneously escape senescence and acquire genomic changes. *Nature* 409:633-637 (2001).

CHROMOSOME ABERRATIONS

	Numerical Aberrations (Chromosome Number)								
	44	45	46	47	48	49	50	polyploid	
Fibroblasts WSt718 Cell Number	1	3	73	1	0	0	1	1	Total Number 80
HMEC WH612/3 Cell Number	1	14	17	10	10	1	2	8	63

	Structural Aberrations (Aberration Type)			
	Apparent Telomere End Associations	[1]Terminal Chromatid Deletions	[2]Dicentric Chromosomes	[4]Double Minutes
Fibroblasts WSt718	0	4	3	0
HMEC WH612/3	2	1	4	2

TABLE 3: Solid Giemsa staining of metaphases derived from untreated fibroblasts in passages 4 to 6 and epithelial cells in passage 5 to 8.

1. Deletion in one arm of sister chromatids in a single metaphase chromosome matched with a finding of a single chromatid fragment
2. Chromosomes with 2 centromeres matched with a finding of an acentric fragment
3. Associated pair of dot deletions; one HMEC cell contained 6 and a second contained 3

Figure 1. Estrogen receptor (ER) immunostaining of passage 8 WH612/3p8 cells following irradiation at passage 7 late log-phase with 30, 60, or 90 rad passed then after 24 hr to 96-well plates and grown to log-phase (L) and confluence (C). Cytoplasmic expression of ER is seen in confluent but not log-phase cells. Radiation dose-dependent cytoplasmic expression of ER is seen in both log-phase and confluent cells.

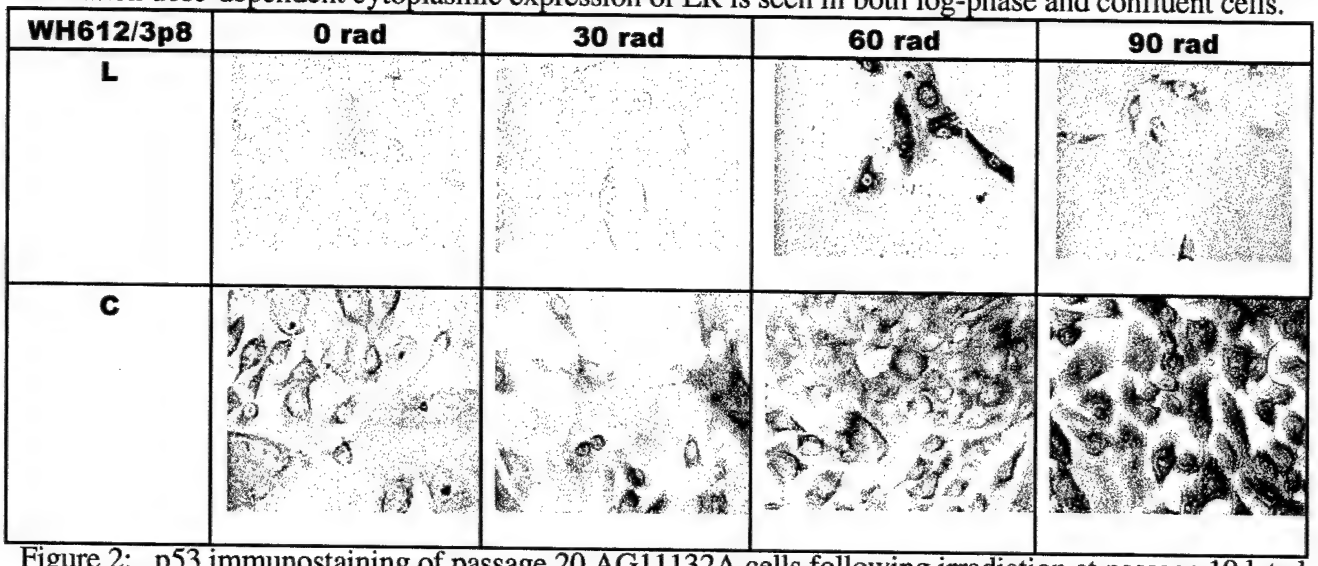

Figure 2: p53 immunostaining of passage 20 AG11132A cells following irradiation at passage 19 late log-phase with 30, 60, or 90 rad passed then after 24 hr to 96-well plates and grown to log-phase (L), late log-phase (LL), and confluence (C). Nuclear expression of p53 is typical in unirradiated C but not L or LL cells. Dose-dependent decrease of p53 nuclear expressions seen in irradiated C cells.

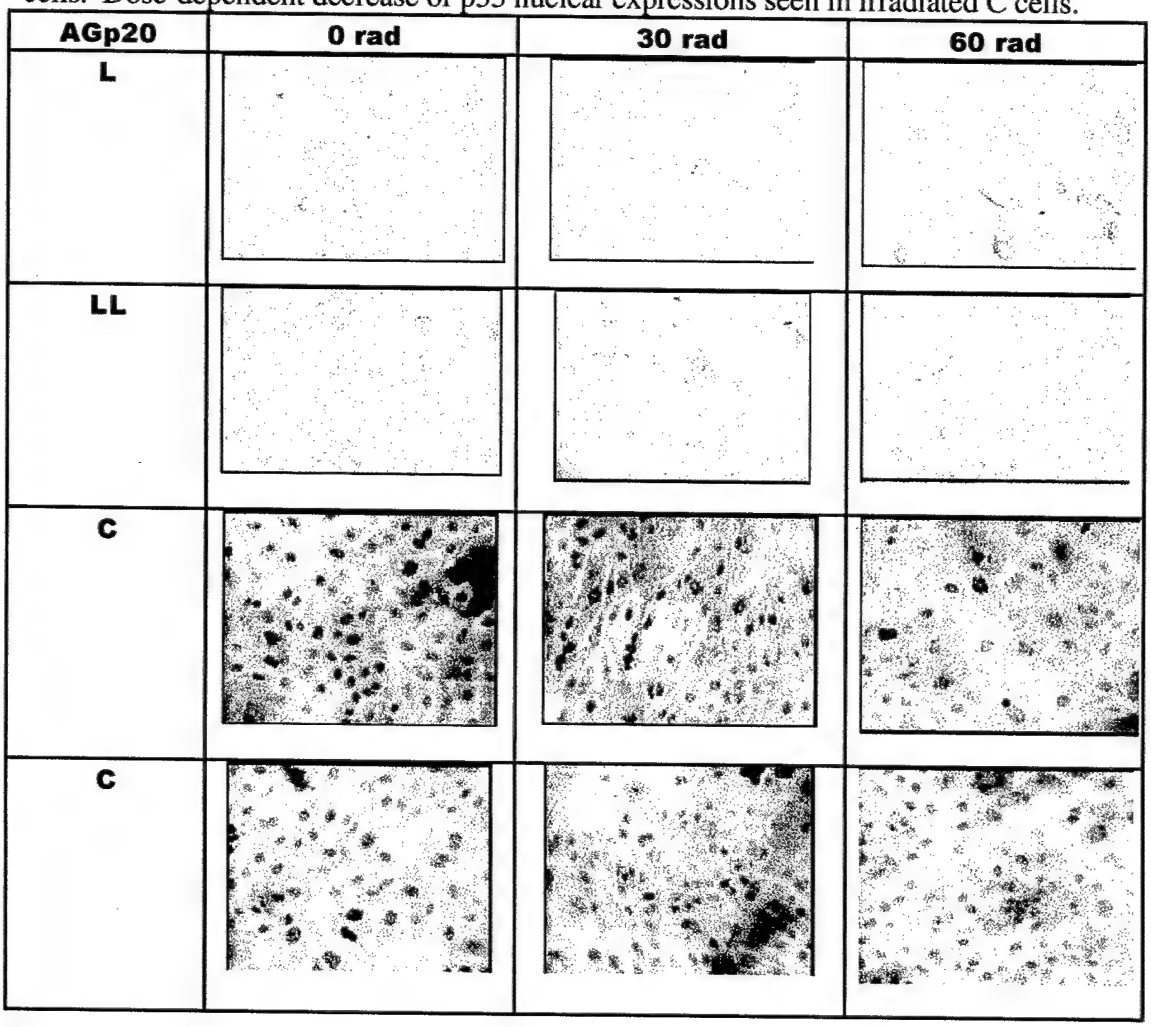

Figure 3: p53 immunostaining of passage 8 WH612/3p8 cells following irradiation at passage 7 late log-phase with 30, 60, or 90 rad passed then after 24 hr to 96-well plates and grown to log-phase (L) and confluence (C). Cytoplasmic expression of p53 is seen in unirradiated but not in irradiated log-phase cells. Dose-dependent cytoplasmic expression of p53 is seen in confluent cells.

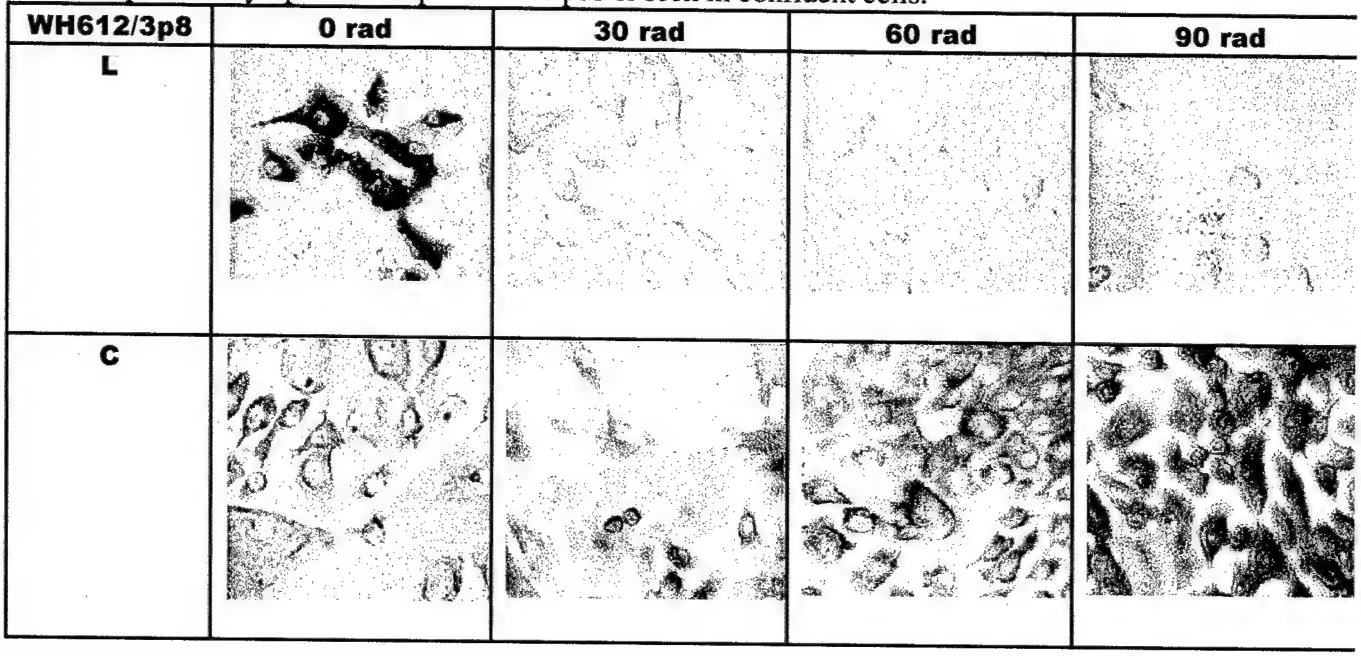

Figure 4: ATM gene-expressed protein (pATM) immunostaining of passage 20 AG11132A cells following irradiation at passage 19 late log-phase with 30, 60, or 90 rad passed then after 24 hr to 96-well plates and grown to confluence (C). Mixed nuclear and cytoplasmic expression of pATM shows radiation dose-dependent decrease.

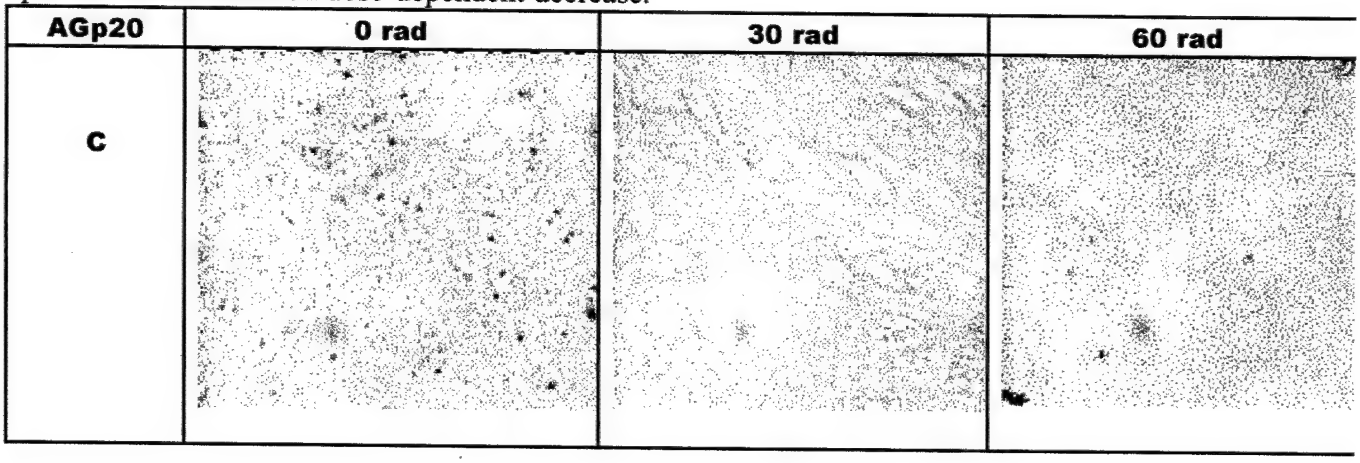

Figure 5: Cytokeratin 18 (CK18) immunostaining of passage 8 WH612/3 cells following irradiation at passage 7 late log-phase with 30, 60, or 90 rad passed then after 24 hr to 96-well plates and grown to log-phase (L), late log-phase (LL), early confluence (EC), and confluence (C). Increasing cytoplasmic CK18 expression in unirradiated cells is seen with increasing cell density. Radiation dose-dependent increase of cytoplasmic CK18 expression is seen in L, LL, and EC cells.

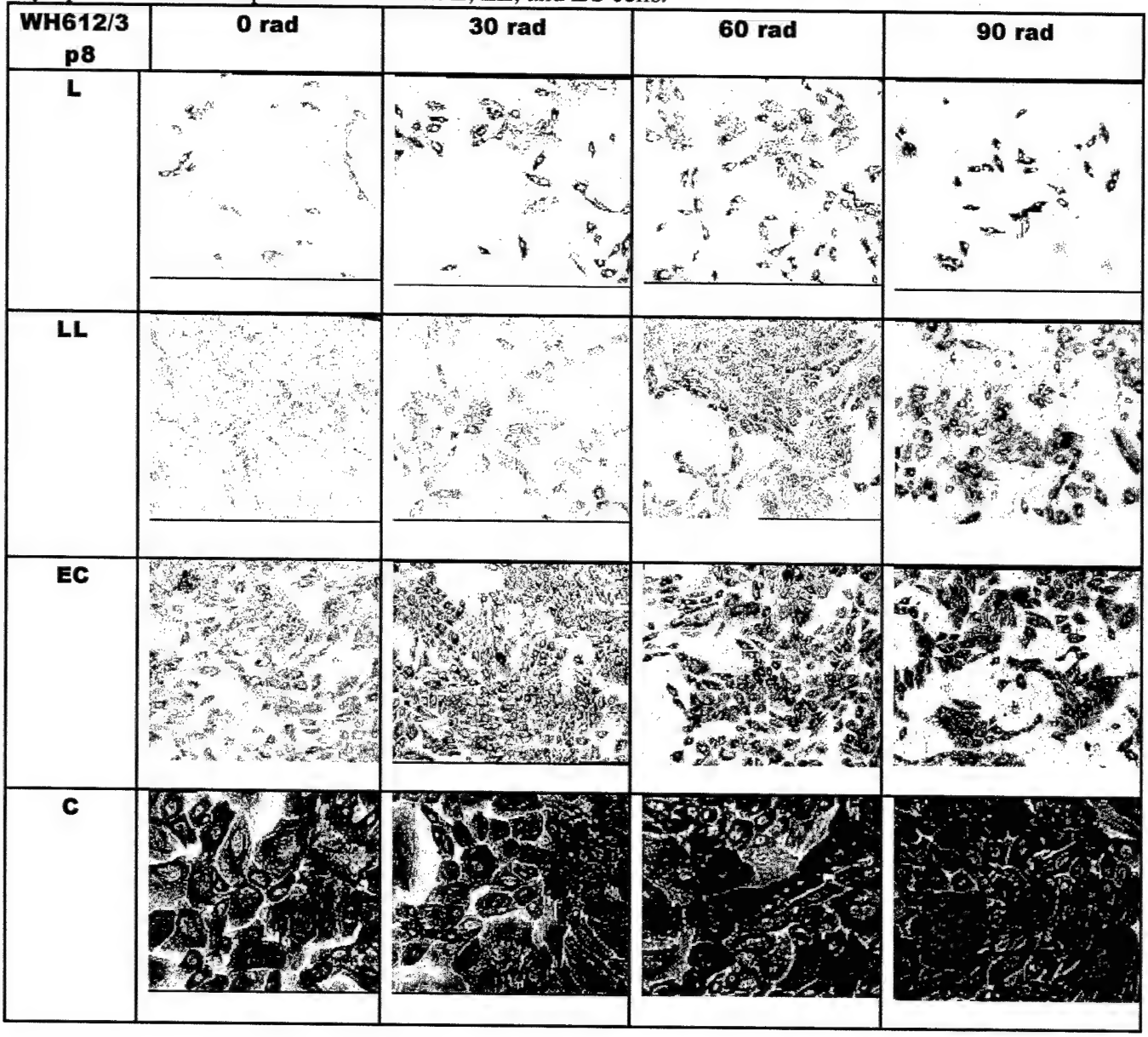

Figure 6: Cytokeratin 18 (CK18) immunostaining of passage 9 WH612/3 cells following irradiation at passage 7 late log-phase with 30, 60, or 90 rad passed then after 24 hr to 96-well plates and grown to log-phase (L), late log-phase (LL), early confluence (EC), and confluence (C). As in Figure 5, increasing cytoplasmic CK18 expression in unirradiated cells is seen with increasing cell density. Radiation dose-dependent increase of cytoplasmic CK18 expression is seen in L, LL, and EC cells.

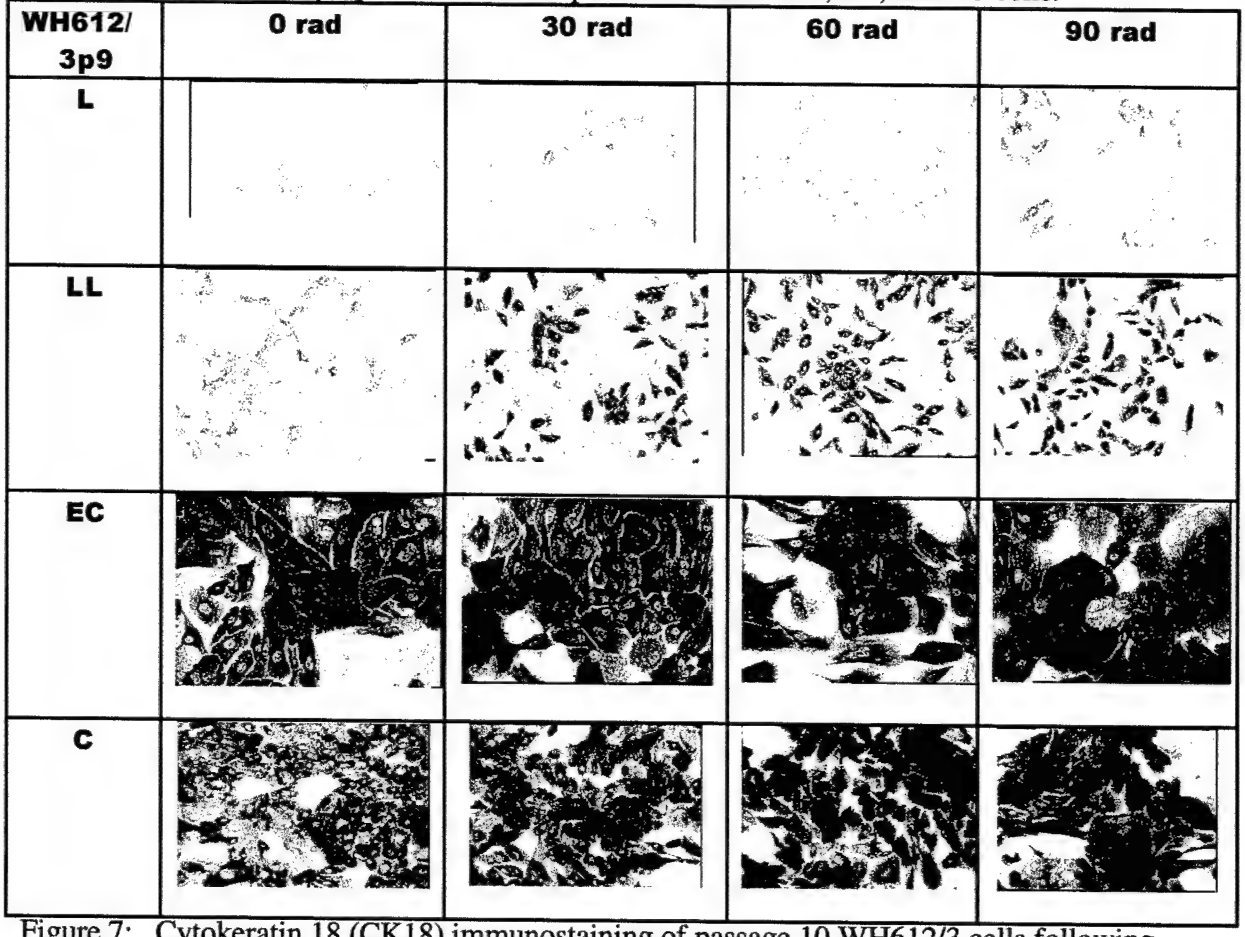

Figure 7: Cytokeratin 18 (CK18) immunostaining of passage 10 WH612/3 cells following irradiation at passage 7 late log-phase with 30, 60, or 90 rad passed then after 24 hr to 96-well plates and grown to log-phase (L) and late log-phase (LL). As in Figure 5, increasing cytoplasmic CK18 expression in unirradiated cells is seen with increasing cell density. Radiation dose-dependent increase of cytoplasmic CK18 expression is seen in L and LL cells.

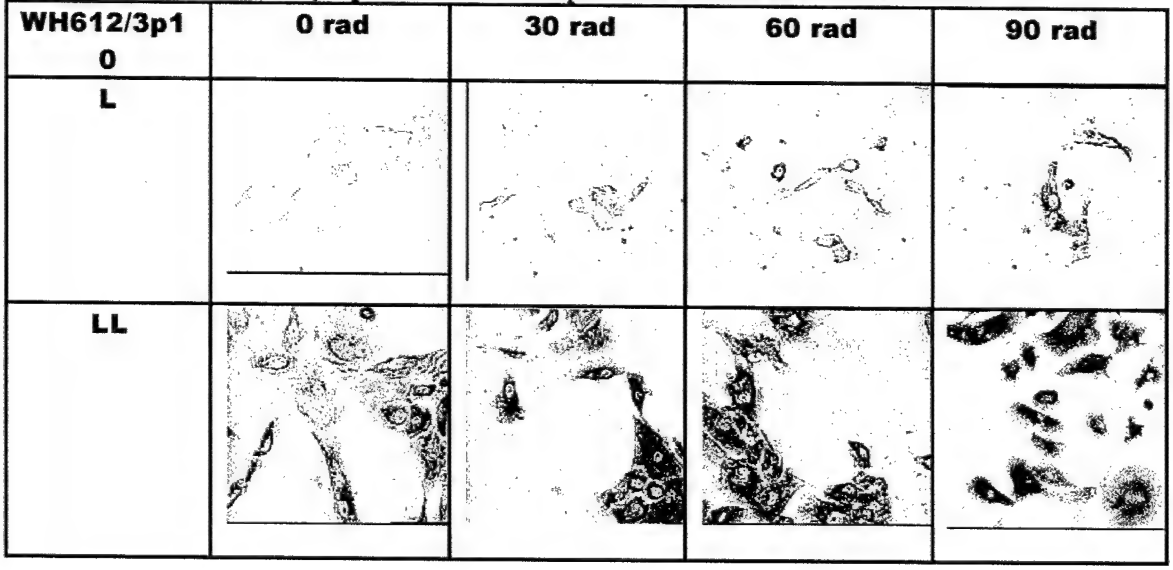

Figure 8: Passage 7 WH612/3 cells irradiated at late log-phase with 30, 60, or 90 rad were successively passed at early confluence in T25 flasks, and at each passage were scored by phase microscopy for the presence of apparent multinuclei. Cells containing apparent binuclei and multinuclei were seen to develop in a passage (age)- and radiation dose-dependent fashion, with results from passage 11 confluent cells detailed The photomicrograph shows the clonal pattern often observed for appearance of bi- and multi-nucleated cells in culture.

	1 X nucleus/cell	2 X nuclear/cell	Average 2X (%)	> 2 X nuclei/cell	Average >2X
0 Rad	244	8 (3%)	3.33% (0.65 SD)	0	0%
	190	6 (3%)		0	
	136	6 (4%)		0	
30 Rad	237	8 (3%)	4.33% (2.3 SD)	0	0%
	165	11 (7%)		0	
	219	6 (3%)		0	
60 Rad	172	14 (8%)	10.00% (1.7 SD)	0	0.67%
	133	15 (11%)		2 (2%)	
	144	16 (11%)		0	
90 Rad	117	25 (21%)	20.33% (8.0 SD)	2 (2%)	3.00% (2.7 SD)
	86	224 (28%)		5 (6%)	
	141	17 (12%)		2 (1%)	

Figure 9: Passage 8 log-phase WH612/3 cells grown 3 days to mid log-phase in complete serum-free media followed by continued 3-day growth in MEGM or replacement with basal growth media MEBM lacking insulin, hydrocortisone, and bovine pituitary extract, after which time cells were stained with trypan blue for subsequent morphometric analysis, and most specifically for the presence of apparent multinuclei in MEBM-grown cells. Apparent multinuclei were seen to develop within greater than 80% of MEBM-grown HMEC, but less than 1% of MEGM-grown cells were binuclear and none were observed with apparent multinuclei.

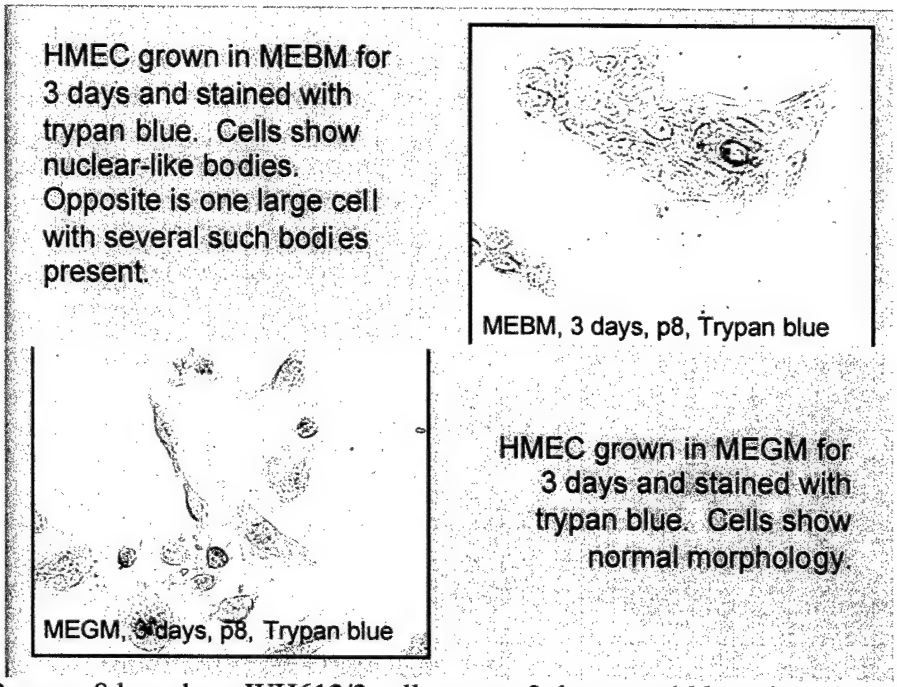

Figure 10: Passage 8 log-phase WH612/3 cells grown 3 days to mid log-phase in complete growth media followed by continued 3-day growth in MEGM or replacement with basal growth media MEBM lacking insulin, hydrocortisone, and bovine pituitary extract, at which time cells were analyzed for TUNEL reaction using FITC-labelled primary mAb. Pronounced TUNEL-positive reaction was seen within the substantial fraction of apparent multinuclei developing within MEBM-grown HMEC, but not within the nearly complete fraction of mononuclei maintained within MEGM-grown HMEC.

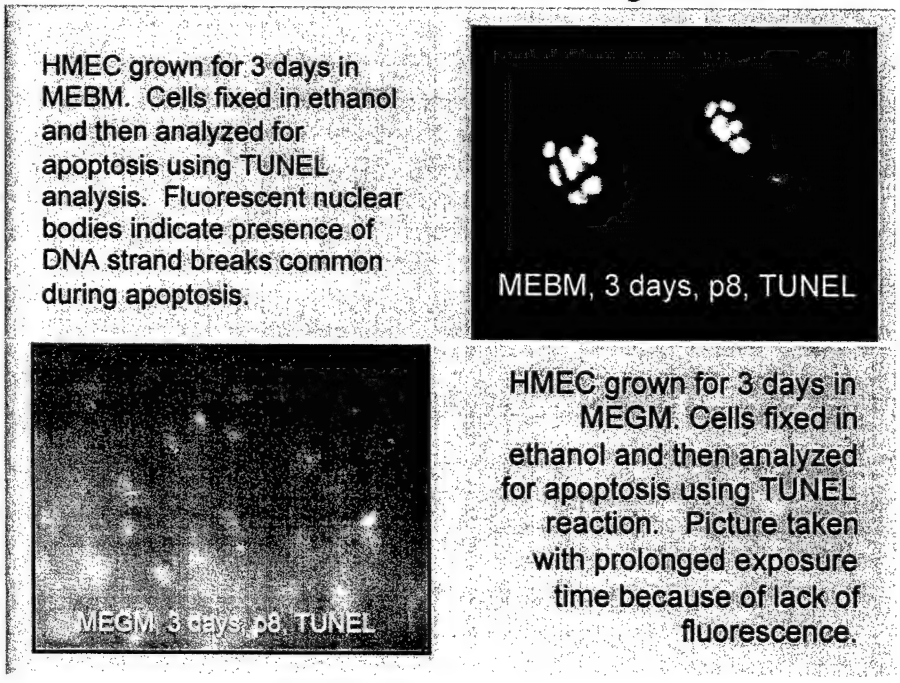

Figure 11: Passage 8 log-phase WH612/3 cells grown 3 days to mid log-phase in complete growth media followed by continued 3-day growth in MEGM or replacement with basal growth media MEBM lacking insulin, hydrocortisone, and bovine pituitary extract, at which time cells were trypsinized and analyzed for DNA-distribution by flow cytometry. A moderate hypoploid fraction and a small hyperploid fraction were seen for cells grown in MEBM. The lack of hyperploidy for MEBM-grown HMEC suggests the apparent multinuclei in these cells observed microscopically (Figures 9 and 10) may be micronuclei that in total retain DNA content contained in the normal nucleus.

MEBM vs. MEGM : Flow cytometer determines hyperploid population

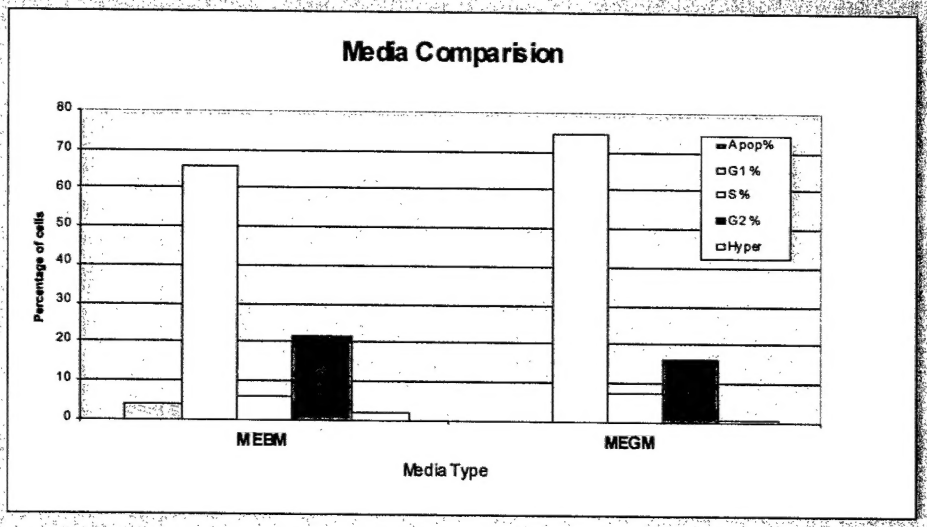

		Hypoploid	G1/G0		S	G2/M		Hyperploid
Media Type	G2/G1	%	Mean	%	%	Mean	%	%
MEBM	1.97	4.27	176.60	66.23	5.90	348.64	22.20	1.88
MEGM	1.94	0.11	191.66	74.55	7.92	371.85	16.42	1.18

Figure 12: Passage 3 WSt718 stromal fibroblasts harvested from A-T heterozygous breast tissue coincident with WH612/3 HMEC. Cells were grown to early confluence, then trypsinized and analyzed for DNA content by flow cytometry. M1: G1 peak of DNA histogram obtained from human mononuclear leukocytes used as normal diploid DNA control. M2: G1 peak from plateau phase of WSt718 fibroblasts. M3: G2/M peak of WSt718 fibroblasts. An increase of mean DNA content by 9.4% is seen in G1 relative to diploid human monocytes, and indicates the degree of DNA aneuploidy in these early passage A-T heterozygous fibroblasts.

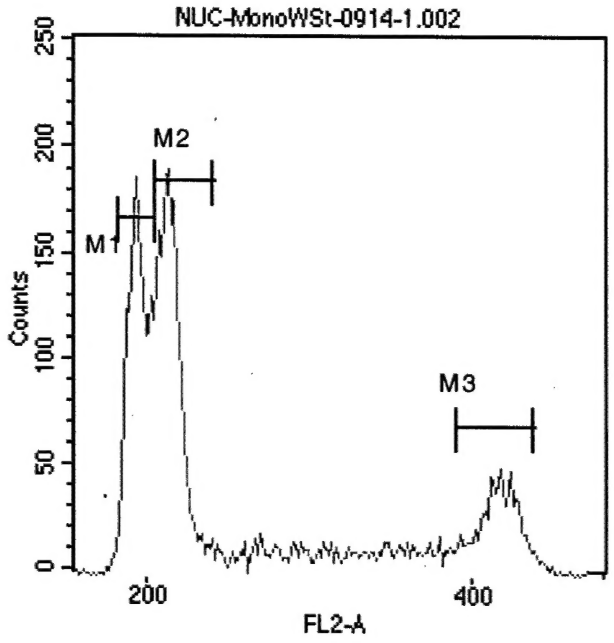

Figure 13: DNA histogram of passage 12 confluent WH612/3 HMEC cells following irradiation in T25 flasks at passage 7 late log-phase with 30, 60, or 90 rad passed then after 24 hr and successively thereafter at late log phase. Open histogram: human monocyte G1-phase diploid standard. M1: G1-phase of cell-cycle; M2: G2-phase of cell-cycle; M3: hyperploid fraction of cell-cycle. DI: DNA-index as monocyte G1 median divided by HMEC G1 median channel numbers.

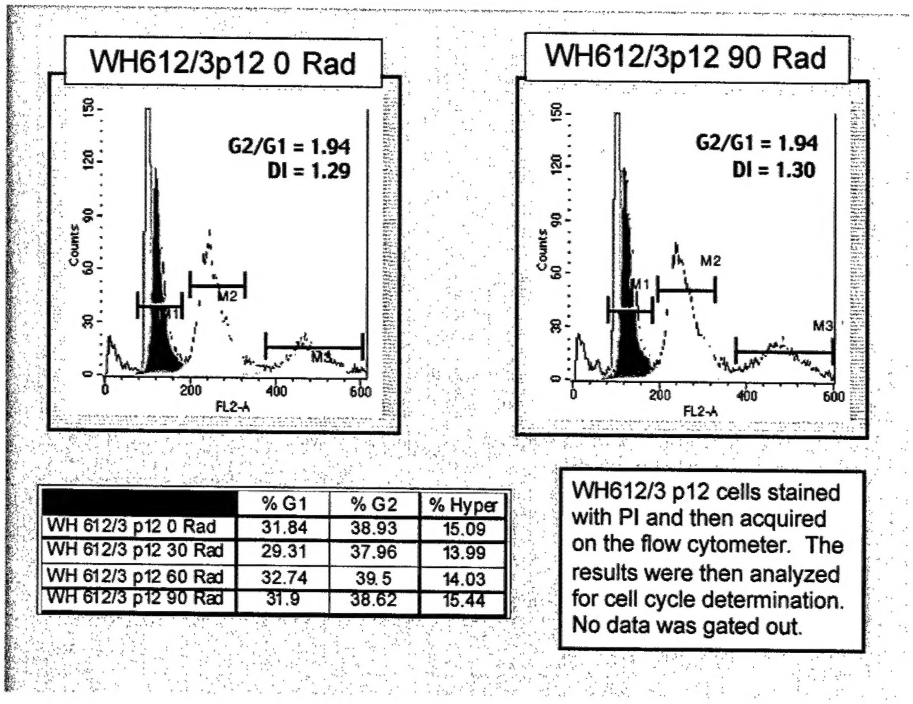

	% G1	% G2	% Hyper
WH 612/3 p12 0 Rad	31.84	38.93	15.09
WH 612/3 p12 30 Rad	29.31	37.96	13.99
WH 612/3 p12 60 Rad	32.74	39.5	14.03
WH 612/3 p12 90 Rad	31.9	38.62	15.44

WH612/3 p12 cells stained with PI and then acquired on the flow cytometer. The results were then analyzed for cell cycle determination. No data was gated out.

Table 4: Tabulation of DNA histogram results of passage 20 confluent AG1113A control HMEC irradiated in T25 flasks at passage 19 late log-phase as detailed for WH612/3 HMEC in Figure 13 legend. Compared to WH612/3 HMEC there is notable differences in absence of hyperploidy and absence of G2-phase accumulation, and notable similarity in lack of radiation-induced alterations of cell-cycle.

	%G1	%G2	%Aneuploidy	%Hyperploidy
AGp20-0Rad	59.10	20.58	28	0
AGp20-30Rad	57.01	19.94	32	0
AGp20-60Rad	56.96	18.22	33	0
AGp20-90Rad	52.88	21.90	35	0

Figure 14: Passage 7 WH612/3 cells irradiated at late log-phase with 30, 60, or 90 rad were successively passed at early confluence in T25 flasks, and at each passage also analyzed for DNA-histogram by flow cytometry. Age (passage)-dependent increase in both G2 accumulation and in hyperploid fraction is observed that is not affected by a history of irradiation.